Effective Spin Hamiltonian and Disorder Effects in Double Perovskite Ferrimagnets

Onur Erten,[1] O. Nganba Meetei,[1] Anamitra Mukherjee,[1,2]
Mohit Randeria,[1] Nandini Trivedi,[1] and Patrick Woodward[3]

[1]*Department of Physics, The Ohio State University, Columbus, Ohio 43210, USA*
[2]*Department of Physics and Astronomy, University of British Columbia, Vancouver, BC V6T 1Z1, Canada*
[3]*Department of Chemistry, The Ohio State University, Columbus, Ohio 43210, USA*

Double perovskites like Sr_2FeMoO_6 are materials with half-metallic ground states and ferrimagnetic T_c's well above room temperature. This paper is the second of our comprehensive theory for half metallic double perovskites. Here we derive an effective Hamiltonian for the Fe core spins by "integrating out" the itinerant Mo electrons. We next validate the classical spin Hamiltonian by comparing its results with those of the full quantum treatment presented in the companion paper "Double Exchange Mechanism for Half-metallic Double Perovskites". We then use it to compute magnetic properties as a function of temperature and disorder. We discuss the effect of excess Mo, excess Fe, and anti-site disorder on the magnetization and T_c. We conclude with a proposal to increase T_c without sacrificing carrier polarization.

Strong electron correlations and the interplay among charge, spin and lattice degrees of freedom lead to a wide range of spectacular phenomena in transition metal oxides[1] such as high T_c superconductivity, colossal magnetoresistance and large thermopower.

Half metals with fully spin polarized ground states provide another example of such unique and spectacular phenomena. Among the known examples, double perovskites (DPs) are of particular interest due to their high ferromagnetic T_c's along with the possibility of integrating different functionalities with oxide electronics[2]. One of the best-studied half-metallic DP is Sr_2FeMoO_6 (SFMO) with T_c=420 K, well above room temperature[2–4]. DPs have the form $A_2BB'O_6$, which is derived from the simple ABO_3 perovskite structure with a three-dimensional (3D) checkerboard ordering of B and B′ ions. DPs have a range of fascinating properties from spin liquids to multiferroics, as well as from metals to multi-band Mott insulators.[2,3,5–7]

This article is the second part of our comprehensive theory for half metallic double perovskites. We begin by summarizing the first paper (hereafter referred to as paper I) titled "Double Exchange Mechanism for Half-Metallic Double Perovskites"[8] where we discuss the full quantum Hamiltonian describing core spins on Fe coupled to conduction electrons through a generalized double exchange mechanism. In paper I, we calculated the magnetic and electronic properties as a function of temperature using exact diagonalization of the "fast" electronic degrees coupled to "slow" core spins configurations generated by classical Monte Carlo simulations (ED+MC). By retaining the electronic degrees of freedom, we obtained information about the temperature dependent density of states and the destruction of the fully polarized half-metallic ground state through thermal fluctuations. One of our central results is that the conduction electron polarization at the chemical potential is directly proportional to the core-spin magnetization. This finding is significant because it indicates that if one can derive an effective Hamiltonian for the core spins, it would be possible to deduce the electronic polarization, a quantity of central importance for spin injection and spin transport, but one that is difficult to measure directly. A second problem the effective Hamiltonian will help ameliorate is the possibility of simulations on large system sizes compared to severe size limitations faced by ED+MC methods.

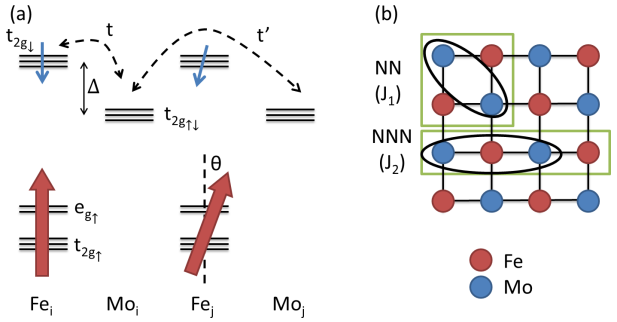

FIG. 1: (a) Schematic showing energy levels at transition metal sites in two unit cells (formula units) of SFMO. The Fe sites have localized $S = 5/2$ core spins, treated as classical vectors with orientation (θ, ϕ). The parameters t, t' and Δ of the Hamiltonian, Eq. (1), governing the dynamics of the itinerant electrons in t_{2g} orbitals, are also shown. (b) Nearest neighbor (NN) and next nearest neighbor (NNN) configuration of two unit cells of DPs.

With this motivation, here we derive the effective Hamiltonian (H_{eff}) for the Fe core spins by integrating out the itinerant Mo electrons. This is a non-trivial generalization of the previous Anderson-Hasegawa analysis for manganites[9] now applied to double perovskites. We validate H_{eff} by comparing the temperature-dependent magnetization M(T) curve with that obtained from the ED+MC method for the full Hamiltonian. We find that the modified double exchange form of H_{eff} indeed captures the magnetic properties of the full Hamiltonian at all temperatures; retaining only Heisenberg interactions works only at intermediate temperatures. It is remarkable that H_{eff} also captures possible metallic antiferro-

magnetic instabilities with increasing carrier concentration. Regarding the effects of disorder, while both excess Fe and Mo decrease the saturation magnetization and T_c, anti-site disorder in which Fe and Mo exchange places, behaves differently; although magnetization drops, T_c is not affected. This finding forms the basis of our proposal to increase T_c without sacrificing conduction electron polarization. Our results suggest that by putting excess Fe and compensating the loss of carriers with La doping can indeed lead to a dramatic increase in T_c.

We start by briefly describing the full quantum Hamiltonian. We then solve the problem of two unit cells and derive the effective exchange Hamiltonian between two Fe core spins. We then generalize this form to the infinite lattice.

For large Hund's coupling J_H, Fe^{3+} in the $3d^5$ configuration saturates the "up" manifold and forms a large spin $\mathbf{S}$=5/2 that we treat classically with a local axes of quantization along $\mathbf{S}_i$. Mo^{5+} ($4d^1$) contributes to conduction in t_{2g} orbitals. Due to the symmetry of t_{2g} orbitals, $d_{\alpha\beta}$ orbitals can only delocalize in $\alpha\beta$ planes[10] ($\alpha\beta = xy, yz, xz$). For all the Mo sites j, we choose the same (global) axis of quantization. The generalized double exchange Hamiltonian[11–13] that describes the core spins interacting with conduction electrons is

$$H = -t \sum_{\langle i,j\rangle,\sigma} (\epsilon_{i\sigma} d^\dagger_{i\downarrow} c_{j\sigma} + h.c.) - t' \sum_{\langle j,j'\rangle,\sigma} c^\dagger_{j\sigma} c_{j'\sigma} + \Delta \sum_i d^\dagger_{i\downarrow} d_{i\downarrow} \quad (1)$$

where $d_{i\sigma}$ ($c_{i\sigma}$) are fermion operators on the Fe (Mo) sites with spin σ.

The orientation (θ_i, ϕ_i) of the classical spins $\mathbf{S}_i$ affects the Mo-Fe hopping via $\epsilon_{i\uparrow} = -\sin(\theta_i/2)\exp(i\phi_i/2)$ and $\epsilon_{i\downarrow} = \cos(\theta_i/2)\exp(-i\phi_i/2)$.

I. EXACT SOLUTION OF TWO SITE PROBLEM

Next we solve the Hamiltonian, Eq. (1) exactly analytically for two unit cells, shown schematically in Fig. 1. This is a generalization of the Anderson and Hasegawa analysis for manganites[9] applied to double perovskites.

In a single unit cell, there are three states derived from the $Fe_\downarrow$ and $Mo_{\uparrow,\downarrow}$ t_{2g} orbitals. We label the unit cells as i and j, and without loss of generality choose a coordinate system such that one of the core spins $\mathbf{S}_i$ is aligned with the z axis, and the other core spin $\mathbf{S}_j$ lies in the x-z plane (Fig. 1(a)). This particular choice of coordinates simplifies the calculation as it gauges away the ϕ dependence. Thus, $\epsilon_\uparrow = \sin(\theta_i/2)$ and $\epsilon_\downarrow = \cos(\theta_i/2)$, where θ is the relative angle between $\mathbf{S}_i$ and $\mathbf{S}_j$. The two unit cell Hamiltonian is given by

$$H = \begin{pmatrix} \Delta & 0 & -t & 0 & 0 & -\gamma t \\ 0 & 0 & 0 & -\sin(\theta/2)t & 0 & 0 \\ -t & 0 & 0 & -\cos(\theta/2)t & 0 & 0 \\ 0 & -\sin(\theta/2)t & -\cos(\theta/2)t & \Delta & t\sin(\theta/2) & -t\cos(\theta/2) \\ 0 & 0 & 0 & t\sin(\theta/2) & 0 & 0 \\ -\gamma t & 0 & 0 & -\cos(\theta/2)t & 0 & 0 \end{pmatrix} \quad (2)$$

in the basis of $\{Fe_{i\downarrow}, Mo_{i\uparrow}, Mo_{i\downarrow}, Fe_{j\downarrow}, Mo_{j\uparrow}, Mo_{j\downarrow}\}$. Here γ=1 for nearest neighbor (NN) and 0 for next nearest neighbor (NNN) configurations (See Fig. 1(b)). By converting the 6×6 matrix for H in a block diagonal form, it can be solved analytically.

The eigenvalues are only a function of the angle between the core spins $\mathbf{S}_i$ and $\mathbf{S}_j$ and describe the effective magnetic exchange Hamiltonians. The lowest eigenvalue for NN configuration, describing one electron in two unit cells corresponding to n=0.5, is

$$H^{\rm FM}_{\rm eff} = -\sqrt{(\Delta/2)^2 + 2t^2(1+\cos(\theta/2))} \quad (3)$$

or equivalently

$$H^{\rm FM}_{\rm eff} = -\sqrt{(\Delta/2)^2 + 2t^2(1+\sqrt{(1+\mathbf{S}_i\cdot\mathbf{S}_j)/2}\,)} \quad (4)$$

where $\mathbf{S}$ is the unit spin vector. We obtain a very interesting modified functional form with a double square root structure that is different from conventional Heisenberg or previously studied Anderson-Hasegawa models[9]. Note that the interaction is ferromagnetic and we calculate the spin stiffness $J_{FM} \equiv \partial^2 E/\partial\theta^2$ by expanding the energy close to $\theta = 0$, where $E(\theta) \approx E(0) + (1/2)(\partial^2 E/\partial\theta^2)\theta^2 + \mathcal{O}(\theta^4)$. We find,

$$J_{FM} \sim \begin{cases} -t & \text{for } t \gg |\Delta| \\ -t^2/\Delta, & \text{for } t \ll |\Delta| \end{cases} \quad (5)$$

showing that the kinetic energy of the conduction electrons sets the scale of the ferromagnetic exchange.

For two electrons in two unit cells, which corresponds to n=1, the effective Hamiltonian is obtained by adding up the lowest two eigenvalues. For the NN configuration, effective Hamiltonian is antiferromagnetic given by

$$H^{\rm AF}_{\rm eff} = -\sqrt{(\Delta/2)^2 + 2t^2(1+\cos(\theta/2))} - \sqrt{(\Delta/2)^2 + 2t^2(1-\cos(\theta/2))}. \quad (6)$$

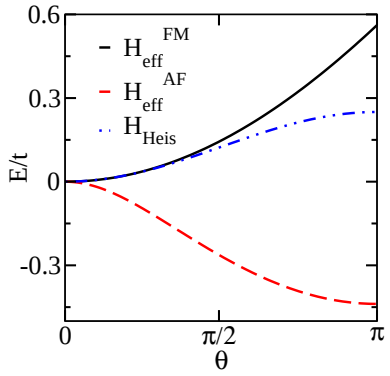

FIG. 2: Energy as a function of θ for ferromagnetic H_{eff} (one electron in two unit cells) and antiferromagnetic H_{eff} (two electrons in two unit cells) . Effective Hamiltonian gives hints for filling dependent magnetic phase transition. We include FM Heisenberg Hamiltonian (H_{Heis}) for comparison. Note that FM H_{eff} is quadratic for a broader range of θ compared to H_{Heis}.

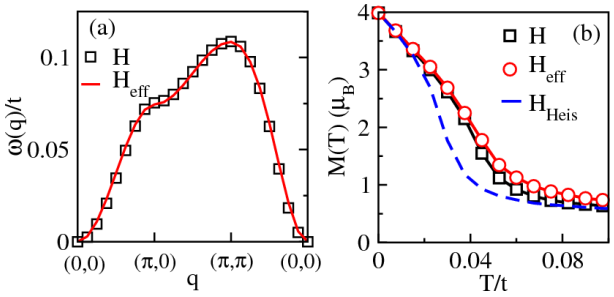

FIG. 3: (a) Spin wave spectrum of full Hamiltonian and the H_{eff}, (b) M(T) comparison between full Hamiltonian, H_{eff}, and Heisenberg Hamiltonian. All simulations are done with an 8×8 system due to the high computational cost of the exact diagonalization and Monte Carlo calculations.

Upon increasing the electron density (n=0.5 → 1), we find that the effective magnetic coupling changes from ferromagnetic to antiferromagnetic which is rather unconventional. The filling driven FM-AFM transition has also been discussed by others[12]. Metallic antiferromagnetism with large local moments at a commensurate wave vector is rare in nature. The exchange stiffness is given by,

$$J_{AF} \sim \begin{cases} t & \text{for } t \gg |\Delta| \\ t^4/|\Delta^3|, & \text{for } t \ll |\Delta| \end{cases} \quad (7)$$

with the scale for antiferromagnetism also set by the kinetic energy of the conduction electrons. Even at a two unit cell level, H_{eff} provides a hint for this transition and illuminates the mechanism, though only discrete fillings are accessible at this level.

II. MAGNETIC PROPERTIES OF THE EFFECTIVE HAMILTONIAN

In this section we use the *ferromagnetic* H_{eff} to calculate the magnetic properties of SFMO. This is justified because SFMO is deep in the ferromagnetic phase and phase competition is not relevant as discussed in paper I [8]. The electronic density of SFMO is n=0.33 and the lowest density achievable in the two unit cell calculation is n=0.5, we will nevertheless use the ferromagnetic H_{eff} form of the NN and NNN exchange interaction generalize it to the infinite lattice

$$H_{\text{eff}} = -J_1 \sum_{\langle i,j \rangle} F_1 \left(\mathbf{S}_i \cdot \mathbf{S}_j\right) - J_2 \sum_{\langle\langle i,j \rangle\rangle} F_2 \left(\mathbf{S}_i \cdot \mathbf{S}_j\right) \quad (8)$$

The function $F_1(x) = 8\sqrt{2+\sqrt{2+2x}}$ is obtained by setting Δ=0 in Eq. (4) for the NN configuration and a similar procedure for the NNN configuration yields $F_2(x) = (5+\sqrt{5})\sqrt{6+2\sqrt{3+2x}}$. By expanding H_{eff} for small θ, we obtain the spin wave spectrum in terms of the exchange constants J_1 and J_2, whose values can now be fitted by matching with the spectrum of the full quantum Hamiltonian, as shown in Fig. 3(a). The agreement over the entire spectral range rather than just at small energies is indeed remarkable. The specific prefactors (8 for F_1 and $(5+\sqrt{5})$ for F_2) are included for convenience to match the spin wave stiffness with that of the Heisenberg model with nearest J_1 and next neighbor J_2 interactions.

Validation of the magnetic H_{eff}: We have performed ED+MC calculations for the full quantum Hamiltonian along with classical Monte Carlo simulations for H_{eff} and for the Heisenberg Hamiltonian. In Fig. 3(b) we present a comparison of the temperature-dependent magnetization M(T) calculated for each of these three Hamiltonians on an 8×8 system. It is encouraging to observe that M(T) calculated from H_{eff} agrees remarkably well with that obtained for the full Hamiltonian *at all temperatures*, whereas the Heisenberg Hamiltonian fails at intermediate temperatures T≃T_c/2. This result gives us confidence in the validity of H_{eff}.

Note that the full quantum model where classical spins are coupled to conduction electrons has low-lying fermionic excitations. If one thinks in a functional integral language, integrating out the fermions would give rise to various extra exchange terms like longer range interactions and four or more spin exchanges. The fact that we can reproduce M(T) at all temperatures shows that the effect of such terms are negligible and we capture the most important magnetic exchange interactions within our model.

The agreement between M(T) for H_{eff} and the full quantum Hamiltonian also indicates that both J_1 and J_2 are temperature independent. Although it is not clear *a priori* why this is the case, the fact that T_c is much less than the bandwidth provides a reasonable justifica-

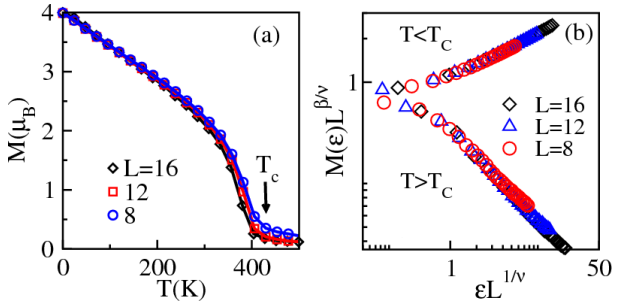

FIG. 4: (a) Magnetization as a function of temperature, M(T), of H_{eff} by classical Monte Carlo calculations for increasing 3D system sizes: 8^3, 12^3 and 16^3. (b) Estimating the thermodynamic T_c using finite size scaling. M(T) for different system sizes collapses to a universal function close to T_c with universal critical exponents. We used $3D$ $O(3)$ universality class exponents and $\epsilon = |T - T_c|/T_c$ is the reduced temperature. As a result, we found T_c=0.14t for SFMO.

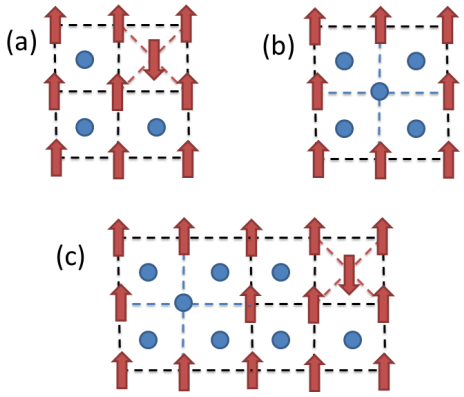

FIG. 5: Types of disorder: (a) excess Fe, (b) excess Mo, (c) anti-site disorder. Black, blue and red lines represent FM bonds, the broken FM bonds and the superexchange between Fe sites.

tion for the temperature independence of the exchange constants up to temperatures of order T_c.

Phase Transition and Determination of T_c: The primary advantage of the classical Hamiltonian H_{eff} is our ability to simulate much larger system sizes compared to those using ED+MC methods. We have performed the first 3D finite temperature simulations of magnetic properties using classical Monte Carlo on up to 16^3 unit cells on an FCC lattice, as shown in Fig. 4(a)). We have determined T_c using the finite size scaling of M(T). According to the finite size scaling hypothesis, $M(T)$ for a system of size L^3 is described by a function of the form $M(T, L) = L^{-\beta/\nu}\mathcal{F}(\epsilon L^{1/\nu})$ where $\mathcal{F}(x)$ is a universal function and $\epsilon = |T - T_c|/T_c$. The critical exponents $\beta = 0.36$ and $\nu = 0.70$ are known for the 3D $O(3)$ universality class. Using T_c as a fitting parameter, we plot $M(\epsilon)L^{\beta/\nu}$ against $\epsilon L^{1/\nu}$ for $L = 8$, 12 and 16. For the true thermodynamic T_c all curves, of different system sizes, collapse onto a single curve, as shown in Fig. 4(b) providing an estimate of $T_c = 0.14t$ for SFMO.

Low temperature spin wave contribution to M(T): Standard ferromagnetic spin waves produce a $T^{3/2}$ reduction of the magnetization, also known as the Bloch $T^{3/2}$ law[14]. However, in Fig. 3(c), M(T) is linear at low T and this linear behavior in fact persists up to a relatively large fraction of T_c. We explain this difference, between the Bloch Law and the calculated linear behavior, as arising from the difference between classical and quantum magnons. The classical Hamiltonian is equivalent to taking the $S \to \infty$ limit of the quantum Hamiltonian but keeping $T_c \sim JS^2$ constant. The $T^{3/2}$ law is restricted to a temperature scale $k_B T_0 \lesssim T_c/S$, the magnon bandwidth or equivalently to $T_0/T_c \sim 1/S$. Therefore the range of temperatures to observe the Bloch law is completely quenched in classical calculations and highly suppressed in the experiment due to the large S=5/2 on Fe.

In order to understand the origin of the linear temperature dependence of the magnetization, we consider the role of spin waves to get

$$M(T) = M_0\Big[1 - \int_{1^{st}\text{B.Z.}} \frac{d^3q}{e^{\beta JSw_q} - 1}\Big] \qquad (9)$$

where the integral is over the first Brillouin zone. For small q, the dispersion for magnons $w_q \sim q^2$. As $S \to \infty$ the exponential can be expanded at all temperatures: $e^{\beta JSw_q} = e^{\frac{\beta T_c w_q}{S}} \approx 1 + \frac{\beta T_c w_q}{S}$ for a constant T_c. Upon using this expansion and evaluating the integral gives $M(T) \sim M_0(1 - \gamma T)$ where $\gamma = \mathcal{O}(1)$. Thus classical spin waves indeed provide a natural explanation of the linear T dependence of the magnetization at low T.

The reason for the robustness of the the linear M(T) dependence up to relatively high temperatures is the peculiar double square root form of H_{eff} (See Fig. 2). Compared to the Heisenberg Hamiltonian, H_{eff} is harmonic ($E \sim J\theta^2$) for a larger domain of θ. Therefore magnon-magnon scattering which is mainly due to the non-harmonic part of the Hamiltonian is highly suppressed and that explains why the spin wave regime and correspondingly the linear T behavior of M(T) survives up to relatively high T. Similar M(T) has been observed in experiments both on single crystals[15] and on thin films[16].

III. DISORDER

In SFMO, there are three common types of disorder: excess Fe, excess Mo and anti-site disorder (See Fig. 5). By using H_{eff}, we perform large scale calculations of the temperature-dependent magnetic properties on systems up to 16^3 to investigate the effects of disorder. Finite size effects close to T_c are highly suppressed with increasing system size as shown in Fig. 4(a). We start the discussion with the general chemical formula $Sr_2Fe_{1+y}Mo_{1-y}O_6$ with y greater (smaller) than zero corresponding to excess Fe (Mo), followed by anti-site disor-

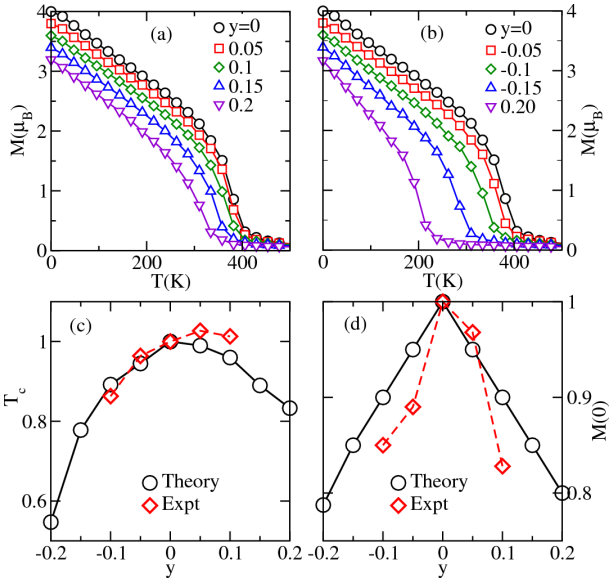

FIG. 6: Effects of Fe & Mo disorder for $Sr_2Fe_{1+y}Mo_{1-y}O_6$ using H_{eff} and comparing it with experiments. (a) Fe rich (y>0) M(T), (b) Mo rich (y<0) M(T), (c) T_c as a function of y, (d) Saturation magnetization, M(0), with y compared with experiments[17].

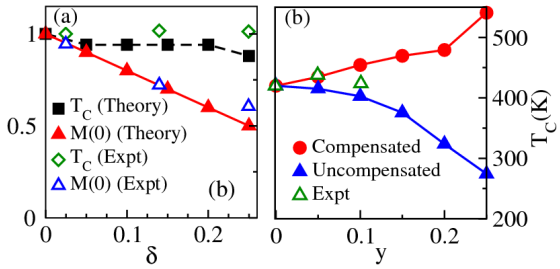

FIG. 7: (a) Anti-site disorder results for T_c and saturation magnetization, M(0) (both normalized with respect to their disorder-free values) compared with experiments, (b) Proposal to increase T_c by La and Fe doping, $La_xSr_{2x}Fe_{1+y}Mo_{1y}O_6$. T_c(y) for compensated (x=3y) and uncompensated (x=0).The uncompensated T_c(y) is compared with experiments[17].

der. We conclude with a proposal to increase T_c without sacrificing conduction electron polarization.

Excess Fe: For y>0, as seen Fig. 5(a) Fe replaces Mo sites which has two main effects: First, it reduces the total conduction electron density that weakens the double exchange mechanism. Secondly, when two Fe sites are close to each other, the strong antiferromagnetic superexchange locks the spins. We estimate the strength of this superexchange $S(S+1)J_{AF} \sim 34$ meV based on T_N=750K for a similar compound $LaFeO_3$ with S=5/2 spins on Fe. The excess Fe spin with the down orientation on the Mo site couples antiferromagnetically to the four neighboring up spins creating a local puddle that *enhances* ferromagnetism in its neighborhood. Capitalizing on this enhanced ferromagnetism will form the basis of our proposal to enhance T_c.

In Fig. 6(a), shows that the saturation magnetization M(0) drops with increasing amount of excess Fe, largely because of its antiferromagnetic coupling to the neighboring Fe sites (see Fig. 6(d)). For small values of y, T_c does not change significantly, then drops rapidly (Fig. 6(d)) beyond y≈ 0.05. The initial insensitivity can be attributed to the changes in T_c from the two effects, reduction of conduction electrons and formation of local ferromagnetic puddles, balancing each other. The behavior of both M(0) and T_c as a function of y are in good agreement experiments[17].

Excess Mo: Excess Mo (y<0) leads to a dilution of the ferromagnetic bonds (see Fig. 5) as well as an increase in conduction electron density. The detrimental effects of dilution and broken ferromagnetic bonds on the magnetization as a function of T shown in Fig. 6(b) is reflected directly in the linear decrease of saturation magnetization M(0) and T_c as a function of y (see Fig. 6(d)). Once again these results are in good agreement with experiments[17]. The behavior of M(0) in off-stoichiometric SFMO is also in agreement with DFT calculations[18].

Anti-site disorder: An example of anti-site disorder (AS) in which Fe and Mo sites replace each others is shown in Fig. 5(c). This is the most prevalent type of disorder in SFMO. It can be thought of as a combination of excess Fe and Mo disorder while keeping the carrier density constant. We quantify AS disorder using δ the fraction of Fe atoms that are on the Mo sublattice; δ=0.5 is a fully disordered system. Fig. 7(a) shows that M(0) drops linearly with a slope of (1-2δ), primarily due to the flipping a Fe spin from the parallel to the antiparallel direction on a Mo site per AS pair, as shown in Fig. 5(c). T_c appears to be insensitive to AS disorder, primarily because two effects balance each other. While the broken FM bonds in the Mo rich regions weakens FM, the puddles of Fe rich regions has the opposite effect. Although Fe sites are coupled antiferromagnetically in these puddles, it locally creates stronger ferromagnetic domains. We believe that these two effects balance each other and T_c does not change significantly with anti-site disorder with very good agreement with experiments[17].

Proposal to increase T_c: We conclude with a proposal to increase T_c without sacrificing conduction electron polarization. We propose adding excess Fe, that locally creates strong ferromagnetic puddles, and simultaneously adding extra La to compensate the loss of carriers. Our results are shown in Fig. 7(b) and suggest that with adequate amount of La doping, T_c can be increased by about 100K.

The general formula for both La and Fe doping is $La_xSr_{2-x}Fe_{1+y}Mo_{1-y}O_6$. Assuming that the Fe valency remains fixed at +3, and only Mo valency changes from +5 to +5+η with doping, the charge balance dictates that η=(2y - x)/(1 -y) or correspondingly, carrier concentration changes from n=1/3 to n = (1 + x - 3y)/3. This implies that y=3x is the necessary amount of La

doping to keep n constant and the result of imposing this constraint is shown in Fig. 7(b). Next we argue that our approach for enhancing T_c is better than only La doping. It is known that La substitution of x = 1 gives rise to a 15% increase of T_c[19]. However, this is accompanied by a huge increase in the extent of anti-site disorder[19]. The effect of La doping x=1, changes the Mo valence from +5 to +4 (using $\eta = -x$). The reduced electrostatic attraction between the Mo and the surrounding oxygen octahedra leads to an expansion of the MoO_6 octahedra. As the volume of the MoO_6 octahedra approaches that of FeO_6, the B-B' ordering becomes fragile[2] and the increased anti-site disorder reduces the polarization significantly[8]. In contrast, our proposal suggests a 25% increase in T_c is obtained for y = 0.25 and x = 0.75, with an average Mo valence of only +4.66 which is unlikely to give rise to large amounts of anti-site disorder.

Finally, we have checked that the proposed system with excess Fe and La compensation is indeed fully polarized at T=0 using ED+MC. The increase in T_c by about 100K is extremely encouraging as that would increase the room temperature polarization significantly.

IV. CONCLUSION

We have found a non-trivial generalization of the double exchange mechanism that is relevant for driving ferromagnetism in the double perovskite half metals. The effective magnetic Hamiltonian H_{eff} with the double square root form, obtained after integrating out the itinerant electrons, is very different from standard Heisenberg or double exchange Hamiltonians and agrees remarkably well when compared with the full quantum Hamiltonian. H_{eff} is found to retain the harmonic θ^2 form in the canting between neighboring spins up to a larger range of θ. As a result classical spin waves provide a good description of the temperature dependent M(T), with suppressed magnon-magnon scattering. We have performed large scale simulations of H_{eff} with different types of disorder. From our insights on the dependence of the saturation magnetization and T_c on disorder, we propose a mechanism to substantially increase T_c by balancing excess Fe doping and compensating the loss of carriers with La doping.

V. ACKNOWLEGMENTS

We thank D. D. Sarma for fruitful discussions. Funding for this research was provided by the Center for Emergent Materials at the Ohio State University, an NSF MRSEC (Award Number DMR-0820414).

[1] M. Imada, A. Fujimori, and Y. Tokura, Rev. Mod. Phys. **70**, 1039 (1998).
[2] D. Serrate, J. M. D. Teresa, and M. R. Ibarra, J. Phys.: Condens. Matter **19**, 023201 (2007).
[3] K.-I. Kobayashi, T. Kimura, H. Sawada, K. Terakura, and Y. Tokura, Nature **395**, 677 (1998).
[4] D. D. Sarma, P. Mahadevan, T. Saha-Dasgupta, S. Ray, and A. Kumar, Phys. Rev. Lett. **85**, 2549 (2000).
[5] G. Chen, R. Pereira, and L. Balents, Phys. Rev. B **82**, 174440 (2010).
[6] G. Chen and L. Balents, Phys. Rev. B **84**, 094420 (2011).
[7] O. N. Meetei, O. Erten, M. Randeria, N. Trivedi, and P. Woodward, arXiv:1205.1811 (2012).
[8] O. N. Meetei, O. Erten, A. Mukherjee, M. Randeria, N. Trivedi, and P. Woodward, Double Exchange Mechanism for Half-Metallic Double Perovskites, Companion paper (2012).
[9] P. W. Anderson and H. Hasegawa, Phys. Rev. **100**, 675 (1955).
[10] A. B. Harris, T. Yildirim, A. Aharony, O. Entin-Wohlman, and I. Y. Korenblit, Phys. Rev. B **69**, 035107 (2004).
[11] J. L. Alonso, L. A. Fernández, F. Guinea, F. Lesmes, and V. Martin-Mayor, Phys. Rev. B **67**, 214423 (2003).
[12] P. Sanyal and P. Majumdar, Phys. Rev. B **80**, 054411 (2009).
[13] O. Erten, O. N. Meetei, A. Mukherjee, M. Randeria, N. Trivedi, and P. Woodward, Phys. Rev. Letters **107**, 257201 (2011).
[14] P. Fazekas, *Lecture Notes on Electron Correlation and Magnetism* (World Scientific, 1999).
[15] Y. Tomioka, T. Okuda, Y. Okimoto, R. Kumai, K.-I. Kobayashi, and Y. Tokura, Phys. Rev. B **61**, 422 (2000).
[16] A. J. Hauser, R. E. A. Williams, R. A. Ricciardo, A. Genc, M. Dixit, J. M. Lucy, P. M. Woodward, H. L. Fraser, and F. Yang, Phys. Rev. B **83**, 014407 (2011).
[17] D. Topwal, D. D. Sarma, H. Kato, Y. Tokura, and M. Avignon, Phys. Rev. B **73**, 094419 (2006).
[18] R. Mishra, O. D. Restrepo, P. M. Woodward, and W. Windl, Chem. Mater. **22**, 6092 (2010).
[19] J. Navarro, C. Frontera, L. Balcells, B. Martinez, and J. Fontcuberta, Phys. Rev. B **64**, 092411 (2001).